Electronic Supplementary Information (ESI)

Layer-to-layer distance determines the performance of 3D bio-electrochemical lamellar anodes in microbial energy transduction processes

*Diego Massazza, Juan P. Busalmen, Rodrigo Parra and Hernán E. Romeo**

Fig. S1 - Electrode processing conditions

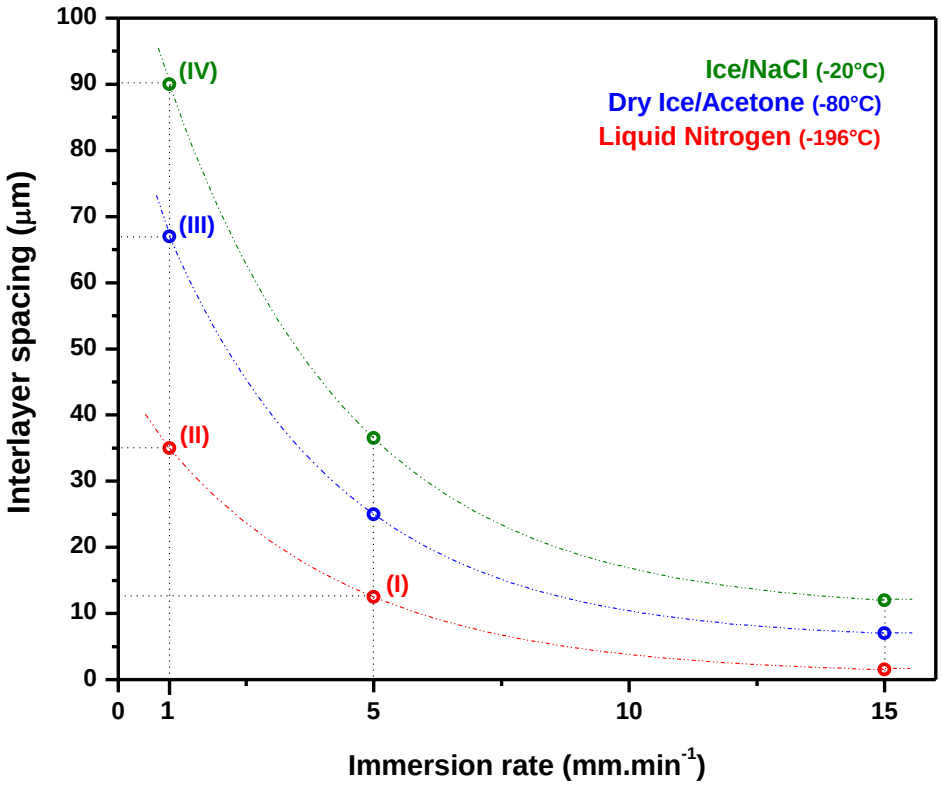

Fig. S1 - Evolution of electrode interlayer separation according to the cooling liquids (the temperature of the liquid source is indicated in brackets) and immersion rates used in the directional freezing technique. Depicted curves are only valid for the aqueous dispersions employed in this study. Any parallel to other systems could lead to deviations, being necessary to reproduce the experimental approach for each particular dispersion. Numbers (I) to (IV) correspond to the experimental conditions used in this study (electrodes prepared according to these conditions are named A, B, C and D, respectively). Each point is representative of three independent measurements.

Fig. S2 - Schematic representation of the experimental set-up

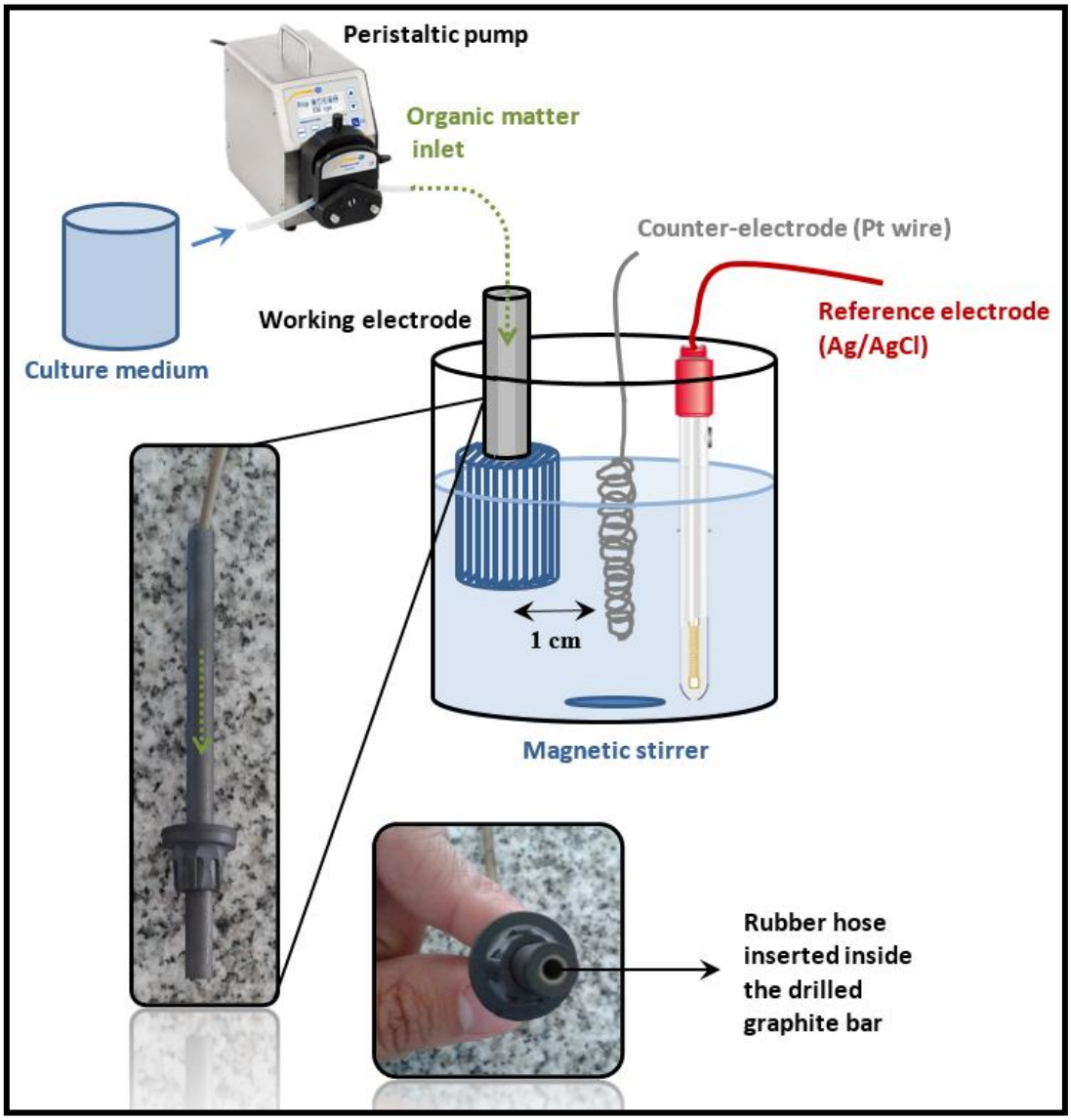

Fig. S2 - Diagram of the experimental electrochemical cell (three-electrode reactor) used. Porous monoliths (working electrodes) were polarized *vs.* Ag/AgCl reference electrode, using a Pt wire as a counter-electrode. Electrical contact of the working electrodes to the external circuit was performed by gluing graphite rods on the porous monoliths, using conducting epoxy adhesive. Graphite rods were prevented from coming into contact with the liquid culture medium. In order to continuously supply fresh medium through the oriented macrochannels, a flow-through system was developed. For this, the graphite bar used to make the external electrical contact was drilled, and a rubber hose (1.5 mm internal diameter) was place in it (this is detailed in the photographs accompanying the diagram). A peristaltic pump was used to inject culture medium through the oriented electrode architectures (the dotted arrow indicates the flow direction). The reactors and all liquid reservoirs were maintained at 32ºC while continuously flushed with a N_2:CO_2 mixture (80:20) to adjust the pH to 7.4 and to prevent oxygen contamination.

Fig. S3 - Relative electrode surface areas

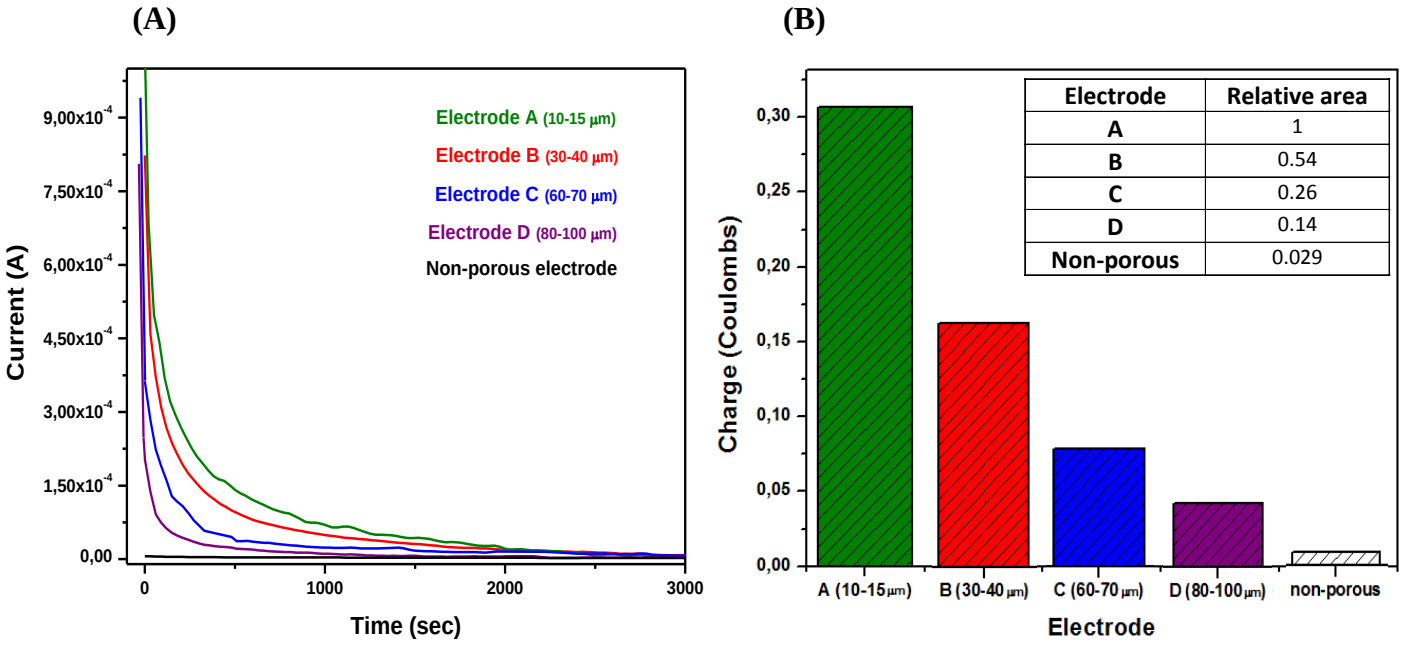

Fig. S3 - (A) Current discharged in time corresponding to the tested electrodes. The area under the curves represents the accumulated charge at the electrode surface/solution interface. **(B)** Bar chart depicting the accumulated charge as a function of layer-to-layer distance for each electrode. The total charge is proportional to the anode surface area. The inset table depicts the resulting relative electrode areas.

Fig. S4 - SEM images of ITTC electrodes

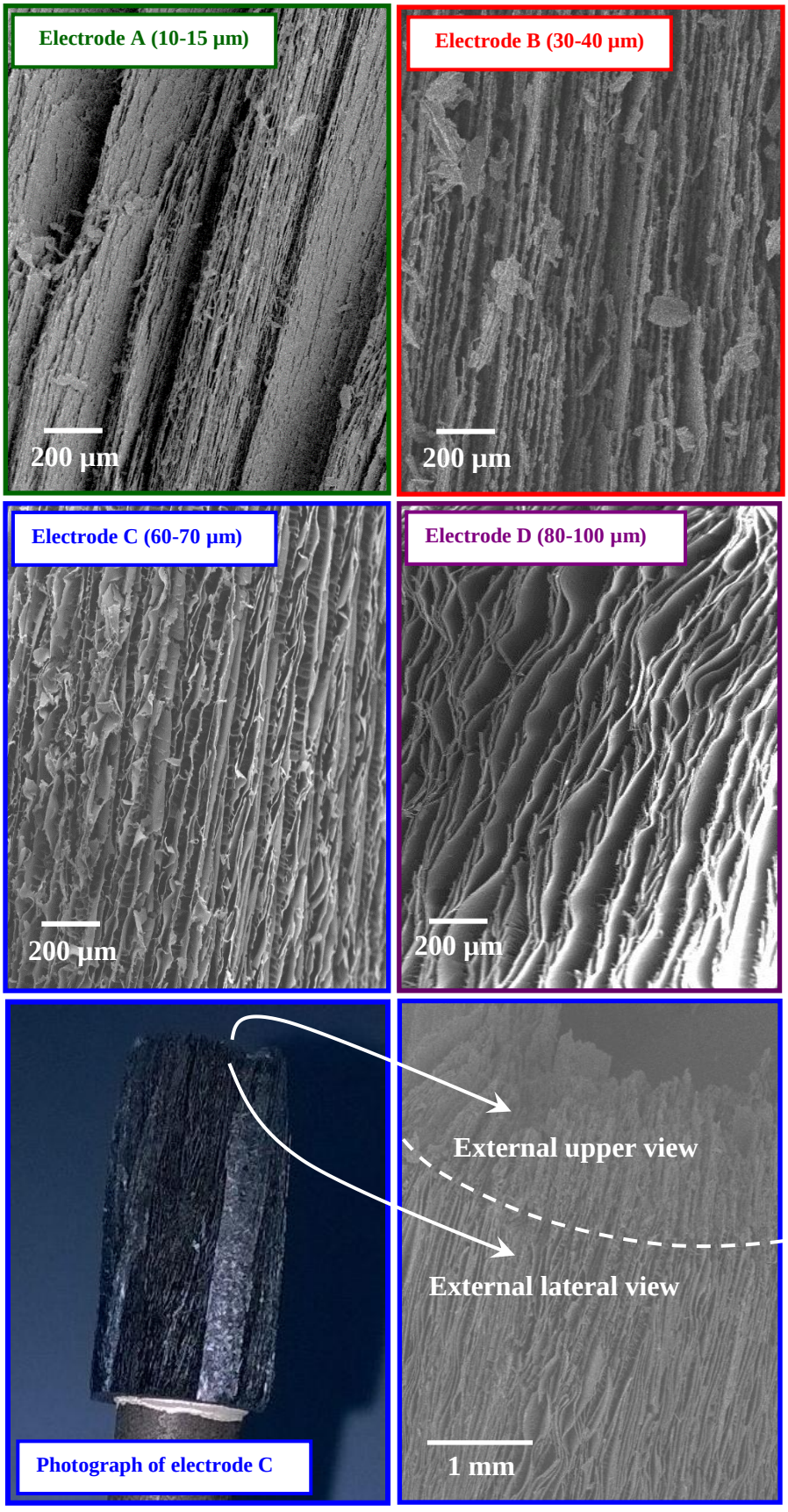

Fig. S4 - Scanning electron micrographs of ITTC bio-anodes. Bottom left: photograph of the electrode C and a SEM image of its external features. The dashed line indicates (as a guide to the eye) the separation between the

lateral and upper parts of the electrode. In all the images, some material debris and lamella irregularities are observed, which are typically produced during the manipulation and preparation for electrode observation.

Fig. S5 - Electrode performance

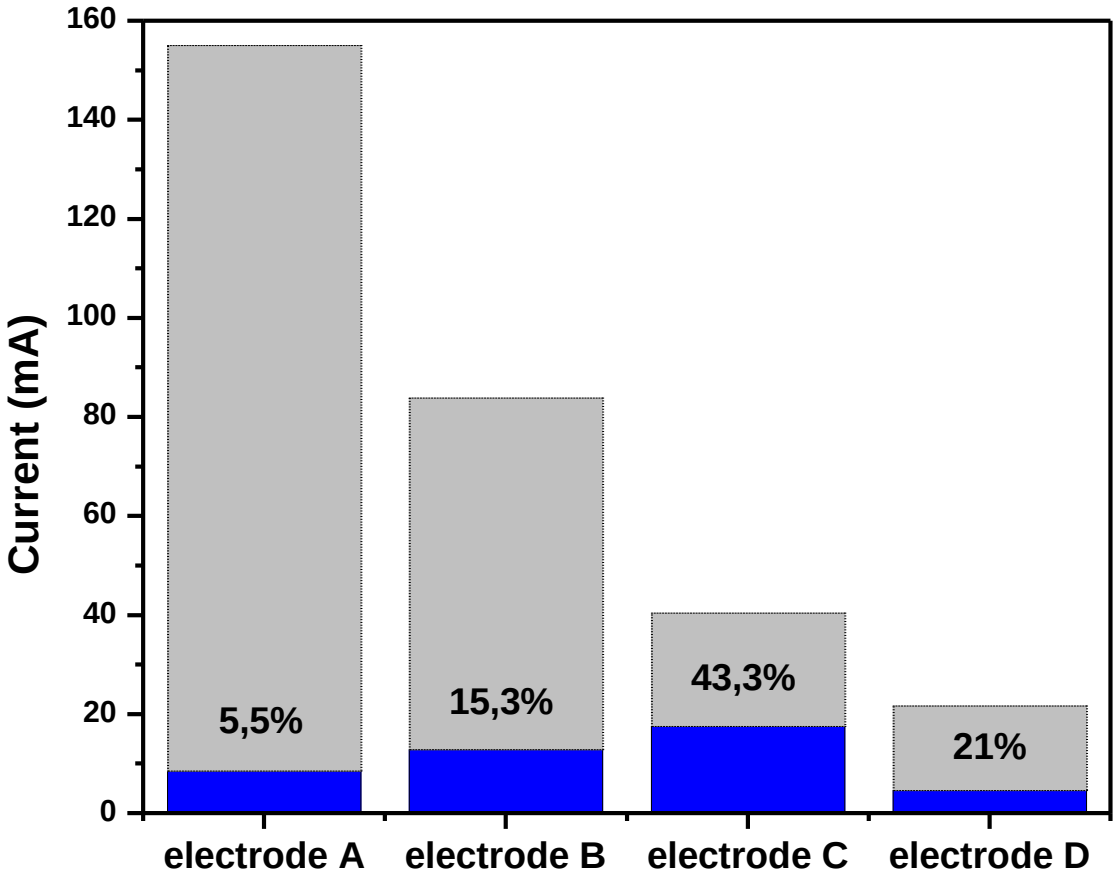

Fig. S5 - Grey-colored bars represent the current that could be ideally reached if scaling the surface current density of the non-porous anode (2 $mA.cm^{-2}$) to each porous electrode according to their relative areas. Blue-colored bars account for the obtained electrical currents.

Fig. S6 - Biofilm thickness

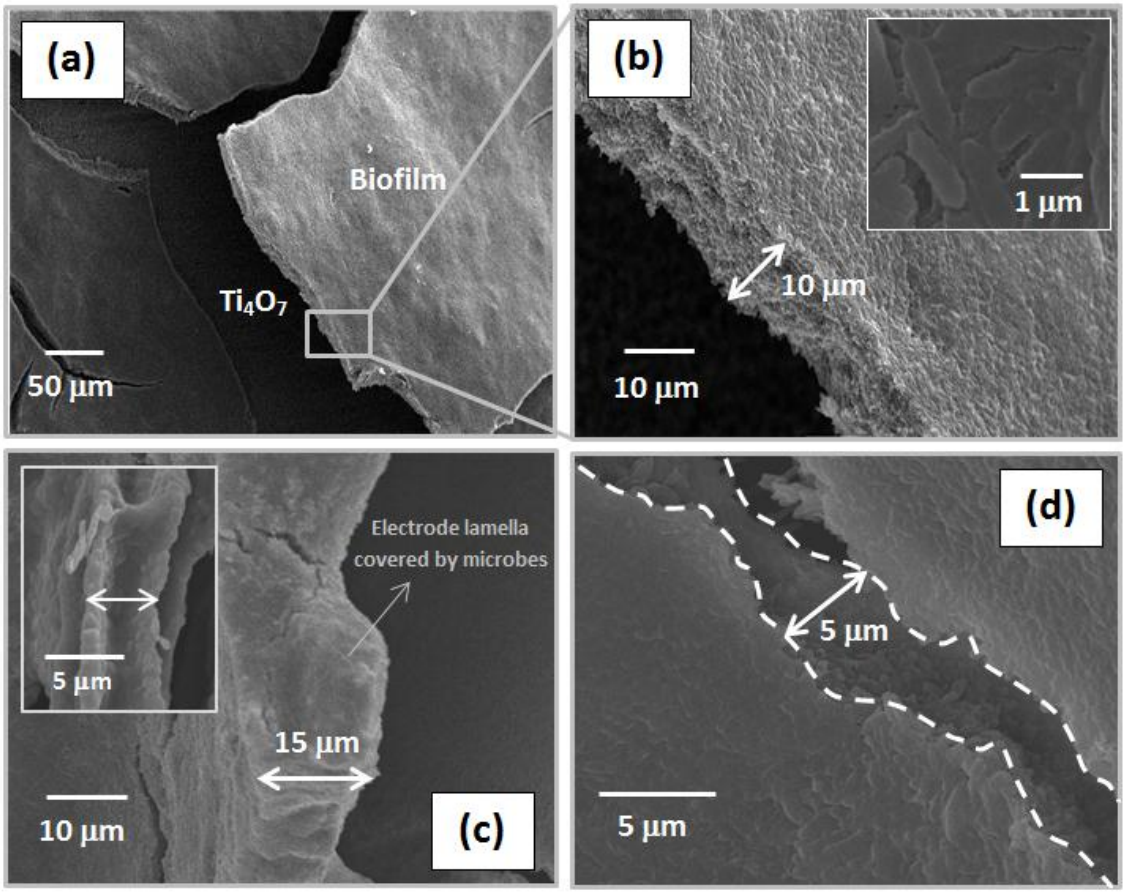

Fig. S6 - SEM micrographs of biofilms evolved on the non-porous electrode and on bio-anode C. **(a)** Biofilm developed on the non-porous Ti_4O_7 electrode, **(b)** magnification of the microbial film shown in (a), **(c)** detail of one lamella of electrode C covered by a film of *G. sulfurreducens*, and **(d)** magnification of the biofilm evolved on the lamella. Inset in (b) depicts a further magnification of the compact biofilm. Inset in (c) shows a detail of a neat lamella, before being colonized by bacteria. According to the naked-wall thickness (~ 5 µm), and considering the microbial covering, a biofilm with half a thickness compared to that on the non-porous electrode was revealed.